it has been pointed out by Chantry (private communication) that the value of electron affinity determined from appearance potentials depends critically on the selection of the leading edge of the negative-ion cross section which one takes as the appearance potential. If one takes the center of the sharply rising part of the $NO^- - NO_2$ cross section from Ref. 15, one obtains $A_e(NO) \geq 3.115 - 3.080$ eV = 0.035 eV, in good agreement with the value of 0.02 eV in Ref. 20.

[16]F. D. Fehsenfeld, E. E. Ferguson, and A. L. Schmeltekopf [J. Chem. Phys. 45, 1844 (1966)] have shown that the charge-transfer reaction $NO^- + O_2 \rightarrow O_2^- + NO$ has an extremely high rate constant ($\sim 9 \times 10^{-10}$ cm^3/sec, which is equivalent to a cross section of about 10^{-13} cm^2). This reaction shows that $A_e(NO) \leq A_e(O_2)$, i.e., $A_e(NO) \leq 0.43$ eV.

[17]A. L. Farragher, F. M. Page, and R. C. Wheeler [Discussions Faraday Soc. 37, 203 (1964)] obtain a value for $A_e(NO)$ of 0.9 eV using the magnetron technique.

[18]J. Jortnev and V. Sokolov [Nature 190, 1003 (1961)] obtain a value of $A_e(NO) = 0.85$ eV and $A_e(O_2) = 0.76$ eV using a spectrophotometric technique.

[19]J. L. Pack and A. V. Phelps, Phys. Rev. Letters 6, 111 (1961); also see J. Chem. Phys. 44, 1870 (1966).

[20]R. Celotta, R. Bennett, J. Hall, M. W. Siegel, and J. Levine, Bull. Am. Phys. Soc. 15, 1515 (1970).

[21]G. V. Calder and K. Ruedenberg, J. Chem. Phys. 49, 5399 (1968).

[22]The approach to this and other empirical formulas by Calder and Ruedenberg uses the fact that one expects electronic potentials to show some regular behavior for diatomics formed from atoms in the same *column* of the Periodic Table. They tabulate the empirical constants relating the spectroscopic constants for combinations of atoms from various columns of the Periodic Table. However, when an additional electron is added to the molecule (effectively moving one of the atoms to a different column), or the molecule is raised to an excited level, the electronic potential of the molecule is changed. The constants which relate to the neutral atoms then no longer strictly apply. For this reason, the value of the anharmonicity calculated from Calder and Rudenberg's formula is probably only accurate to within about 20%.

[23]R. M. Badger, J. Chem. Phys. 2, 128 (1934); 3, 710 (1935).

[24]P. M. Morse, Phys. Rev. 34, 57 (1929).

[25]G. Herzberg, *Spectra of Diatomic Molecules* (Van Nostrand, Princeton, N. J., 1967).

[26]F. R. Gilmore, J. Quant. Spectry. Radiative Transfer 5, 369 (1965).

[27]For a qualitative description of shape resonances see H. S. Taylor, G. V. Nazaroff, and A. Golebiewski, J. Chem. Phys. 45, 2872 (1966).

[28]J. M. Blatt and V. F. Weisskopf, *Theoretical Nuclear Physics* (Wiley, New York, 1952), p. 360.

[29]L. M. Chanin, A. V. Phelps, and M. A. Biondi, Phys. Rev. 128, 219 (1962).

[30]A. Herzenberg, J. Chem. Phys. 51, 4942 (1969).

PHYSICAL REVIEW A VOLUME 3, NUMBER 6 JUNE 1971

Differential Spin Exchange and the Elastic Scattering of Low-Energy Electrons by Potassium†*

R. E. Collins,‡ B. Bederson,§ and M. Goldstein‖
New York University, University Heights, New York, New York 10453
(Received 27 August 1970)

Results are reported on the elastic scattering of low-energy electrons by potassium. The atomic-beam crossed-beam recoil technique is used, with velocity selection and spin selection and analysis of the atom beam. The results include total, differential, and differential spin-exchange cross sections, in the energy range 0.5–1.2 eV. Comparison is made with close coupling, as well as with adiabatic-type calculations. Additional total cross-section measurements up to 9 eV are also presented. These are significantly smaller and lack the pronounced structure of the early results of Brode.

I. INTRODUCTION

Rubin, Perel, and Bederson[1] developed a novel method for the study of low-energy electron-atom collisions with spin analysis. In this method, called the "recoil technique," observation of the interaction is made on the scattered atoms rather than the electrons.[2] The recoil scattering angles are generally quite substantial and as a consequence the method can be used to study both differential scattering, by collecting atoms scattered away from the beam axis (scattering-in), and total scattering, by noting the attenuation of the full atom beam when cross fired by electrons (scattering-out). In the latter mode an absolute value of the cross section can be obtained from knowledge of the electron current, the atom-beam mean speed, and geometry factors; knowledge of the *neutral* beam density is not required.

Scattering experiments can also be performed with state selection before the interaction, and state analysis after the interaction. For example, using the alkalis in strong magnetic fields, one can spin align the atomic beam and, after scattering, a spin analysis can be performed on the scattered atoms. This procedure yields the spin-flip

cross sections as a function of recoil scattering angle since the analysis is capable of sampling a small range of recoil scattering angles at a time. If only elastic scattering can occur, and provided spin-orbit interactions can be neglected during the interaction, this is the same as the differential spin-exchange cross section $\sigma(\theta)_{ex}$, measured as a function of electron energy and atom scattering angles, which can be transformed to the electron polar scattering angle provided the atom beam has been velocity selected. Such a procedure is similar in concept to analogous experiments performed by Kleppner and Pritchard *et al.*[3] involving atom-atom, rather than electron-atom interactions. Rubin *et al.*[1] attempted to measure the differential cross section $\sigma(\theta)$ as well as $\sigma_{ex}(\theta)$ for potassium. As a consequence of experimental limitations the exchange cross sections were presented as upper and lower bounds.

The present work employs a new atomic-beam apparatus which, combined with greatly improved electron-beam technology and data-processing procedures enabled us to obtain quantitative results on elastic scattering by potassium, with reasonable over-all experimental error. Specifically we report here on measurements of the ratio $\sigma_{ex}(\theta)/\sigma(\theta)$ for potassium for four energies below the first threshold for excitation (0.5, 0.75, 1.0, and 1.2 eV), absolute values of $\sigma_{ex}(\theta)$ and $\sigma(\theta)$ obtained by normalizing the relative results to an absolute total cross-section measurement, and total absolute cross sections σ in the energy range 0.4–9.0 eV. Our results are compared with values recently calculated by Karule and by Karule and Peterkop in a close-coupling approximation.[4,5]

II. THEORY OF DIFFERENTIAL MEASUREMENTS

Details of the recoil method are presented in a recent paper by Rubin, Bederson, Goldstein, and Collins (RBGC).[6] We discuss very briefly here aspects of the method which pertain specifically to elastic differential scattering. A polarized and velocity-selected potassium beam is cross fired by a modulated electron beam. Recoiled atoms are spin analyzed and detected by an assembly which rotates about the scattering center in the plane of the two beams. This detector accepts only those atoms which are scattered into a narrow range of angles $\Delta\psi$ about ψ, the atom scattering angle in this plane. (The electron and atom scattering angles are shown in Fig. 1.) The scattering signal is related to the differential cross section $\sigma(\theta)$ through the conservation-of-momentum equations, apparatus geometry factors, and integrations over the electron- and atom-velocity distribution functions and beam profiles.

In the present analysis we neglect the spread in atom velocities and assume a "pencil" atom beam of negligible height and width. RBGC then show that the scattering signal $S(z)$ at the detector position z is

$$S(z) = \text{const} \times \int dE \, \frac{N(E)\gamma(\theta, E)\sigma(\theta, E)}{E^{1/2}}, \qquad (1)$$

where ψ and z are related by $z = \psi L$, and L is the distance between detector and scattering region. The constant includes various geometry and beam factors, which are in principle calculable. However, to obtain absolute values of $\sigma(\theta)$ we essentially *measure* the constant in an auxiliary calibration experiment (see Sec. VII). $N(E)$ is the electron energy distribution experimentally determined from retarding-potential measurements.

$\gamma(\theta, E)$ is called the "azimuthal form factor" (AFF). It represents the fraction of all atoms scattered into $\Delta\psi$ which are detected at ψ as a consequence of the finite detector height. In the approximation that $\alpha = mv/MV \ll 1$, where mv, MV are the electron and atom momenta, respectively, it is easy to show that all atoms scattered into (θ, φ) are scattered into the same ψ, to first order in ψ. However, different φ's correspond to different χ's (Fig. 1). A detector of height $h \geq 2\alpha L$, assuming no beam obstructions (e.g., collimating slits and finite dimensions of the analyzing magnet gap), would then collect all atoms

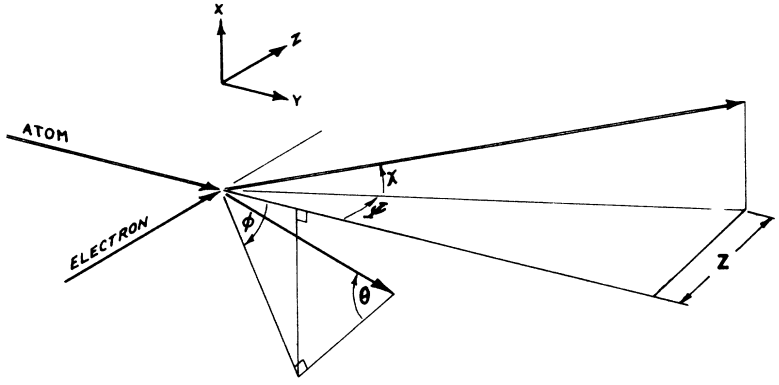

FIG. 1. Definitions of atom and electron scattering angles. The electron azimuthal angle φ is measured with respect to the plane defined by the two incident beams.

scattered into $\Delta\psi$. For such a system $\gamma = 1$. Ordinarily, because of the analyzer magnet, $\gamma \ll 1$ except for angles corresponding to $\theta \approx 0°$ and $\approx 180°$. For a pencil beam the analytic forms for the AFF are

$$\gamma(\theta) = 1, \qquad \sin\theta < h/2\alpha L$$
$$\gamma(\theta) = 1 - \frac{2}{\pi}\cos^{-1}(h/2\alpha L \sin\theta), \qquad \sin\theta > h/2\alpha L \tag{2}$$

where h is the detector height (assuming no obstructions). Figure 3 of Ref. 6 shows plots of $\gamma(\theta)$ for 1-eV electrons and a potassium beam for both a monoenergetic electron beam and for an electron beam averaged over its observed energy spread.

A corresponding equation to Eq. (1) can be written for the exchange signal $S_{ex}(z)$, the scattering signal at z for atoms which have suffered change of spin state during collisions with the electron beam. All quantities in this expression will be the same, except $\sigma(\theta)$ is replaced by $\frac{1}{2}\sigma_{ex}(\theta)$. This assumes that the spin analyzer possesses a unit transmission efficiency, i.e., passes all atoms with reversed spin states with the same efficiency as when it is inoperative. (The influence of the transmission of the analyzer is discussed in Appendix A.) The factor $\frac{1}{2}$ appears multiplying $\sigma_{ex}(\theta)$ since only half of the electron beam, consisting of those electrons with spins polarized opposite to the polarized atom beam, participates in this exchange measurement. Exchange events by electrons oriented parallel to the atom beam are unobservable, and are not counted in the signal S_{ex}. We will assume that $\sigma(\theta)$ and $\sigma_{ex}(\theta)$ are slowly varying functions of E (or equivalently, we seek values for σ and σ_{ex} averaged over E). Then we have

$$\sigma(\theta_0, E_0) = \frac{S(z)}{\text{const} \times \int dE\, \gamma(\theta, E) N(E)/E^{1/2}}, \tag{3}$$

$$\tfrac{1}{2}\sigma_{ex}(\theta_0, E_0) = \frac{S_{ex}(z)}{\text{const} \times \int dE\, \gamma(\theta, E) N(E)/E^{1/2}}. \tag{4}$$

Since the denominators of Eqs. (3) and (4) can be evaluated as a function of E, apart from the constant, relative curves for $\sigma(\theta, E)$ and $\sigma_{ex}(\theta, E)$ can be obtained from measurements of $S(z)$ and $S_{ex}(z)$.

The cross sections are related to the appropriate scattering amplitudes by

$$\sigma(\theta, E) = \tfrac{3}{4}|f - g|^2 + \tfrac{1}{4}|f + g|^2, \tag{5}$$

$$\sigma_{ex}(\theta, E) = |g|^2, \tag{6}$$

where f, g are the direct and exchange amplitudes, respectively. These are related to T, S (the triplet and singlet amplitudes) by

$$f = \tfrac{1}{2}(S + T), \quad g = \tfrac{1}{2}(S - T).$$

The simplest quantity to measure in our experiment is the ratio R, defined by

$$R \equiv \sigma_{ex}(\theta)/2\sigma(\theta) = S_{ex}(z)/S(z),$$

since in this determination the complicated denominators of Eqs. (3) and (4) cancel. The systematic errors in the ratio measurement are thus considerably reduced and are primarily the result of errors in the employment of the polarization analyzer and in the assumption that the cross sections are slowly varying functions of the energy. The method used to obtain absolute values of $\sigma(\theta)$ and $\sigma_{ex}(\theta)$ is described in Sec. VI.

In order to obtain relative values of $\sigma(\theta)$ and $\sigma_{ex}(\theta)$ separately, the integral

$$\int dE \frac{\gamma(\theta, E) N(E)}{E^{1/2}}$$

is evaluated numerically, using the experimental electron energy distribution and the AFF calculated on the assumption of a pencil beam with the relevant apparatus dimensions.

III. APPARATUS AND EXPERIMENTAL METHOD

The apparatus has been described by RBGC (see Fig. 1 of Ref. 6). The vacuum envelope consists of three separately pumped stainless-steel chambers joined by two magnet assemblies. These are connected by flexible stainless-steel bellows, permitting independent movements of all components. The polarizer is a Stern-Gerlach magnet which serves to both polarize and velocity select the potassium beam. The velocity resolution of a Stern-Gerlach magnet $\Delta V/V$ can be shown to be approximately equal to $2w/S$, where w/S is the ratio of source slit width to source displacement from the beam axis.[7] In the present experiment $\Delta V/V$ is about $\pm 10\%$. The beam is about 98% polarized as it enters the interaction region. The analyzer is an E-H gradient balance magnet[8] adjusted so that when operative it passes only those atoms which have changed their spin states. The analyzer-detector assembly is constructed so that it can rigidly rotate about the scattering center in the plane defined by the direction of the two incident beams while the detector is capable, in addition, of undergoing independent translation motion, in order to study beam profiles.

The most critical element in this experiment, from the point of view of obtaining reliable data, is the electron gun. It must be capable of producing a beam of reasonable energy spread, and a mean energy which can be reliably determined, reasonably unidirectional with minimal secondary and reflected electrons in the interaction region, accurately positioned, and with properly designed anode to ensure that all electrons which pass through the atom beam are collected and measured. Finally, because of the small probability of scattering into a solid-angle range subtended by the de-

tector when positioned off-axis, the currents must be reasonably large (of the order of tens of μA); this latter requirement precludes the use of monochromatic electrons at the present stage of development of the recoil technique.

A detailed description of the design and operation of this gun is contained in an article published elsewhere.[9]

The current density in the scattering region was always less than 50 $\mu A/cm^2$. The gun produces a uniform parallel beam of electrons of cross-sectional area 0.08×2.54 cm, possessing an energy spread under normal operating conditions (with absolute energies between 0.5 and 3.0 eV) of about 0.25-eV full width at half-height. A strong magnetic field parallel to the electron motion serves to collimate the electrons and to decouple the nuclear and electron spins in the scattering region. The absolute energies determined by retarding potentials agree well with those obtained by observing the onset of inelastic scattering corresponding to $\theta = 0°$. This determination, depending solely upon conservation of linear momentum and knowledge of the atom-beam speed, is an independent method of determining absolute electron energy above the first excitation threshold[6] (1.6 eV in potassium). (A complete discussion of space-charge effects, retarding-potential measurements, and other properties of the scattering gun is contained in Ref. 10.)

IV. STATE AND VELOCITY SELECTION AND ANALYSIS

The pole pieces of the polarizer and analyzer magnets are machined to follow the equipotential surfaces of a two-wire field with a gradient-to-field ratio of 10 cm^{-1}. The pole pieces of the E-H gradient magnet (analyzer) must sustain a potential difference of about 10 kV. The edges of the ceramic insulators which separate the pole pieces are slotted to decrease electrical leakage. After prolonged use a leakage current of 30 μA at 6000 V develops, which we attribute to a thin potassium coating which forms on the insulator surfaces. Both electric and magnetic fields of the analyzer are controlled by servomechanisms in order to achieve long-term stability as well as uniform and reproducible magnetization and demagnetization cycles. The operation of the polarizer-velocity selector (Stern-Gerlach magnet) and the analyzer (E-H gradient balance magnet) are described in RBGC. The error introduced in the measurements of $\sigma_{ex}(\theta)$ by spin-state impurity is between 1–2% and thus does not contribute significantly to the over-all errors of the experiment. During the course of a measurement the electric and magnetic fields in the analyzer have to be switched on and off frequently. The circuits which performed this operation, and the sensor devices which enable reliable and stable reproducibility of these operations, are described in Ref. 10. The magnetic field was controllable to about 0.5%, and the electric field to better than 0.2%.

V. DETECTION AND DATA PROCESSING

A block diagram of the detection system is shown in Fig. 2. The output of the electron multiplier is fed into a 10^8-Ω resistor at the input of a Keithley 603 electrometer. Beam-intensity measurements are made directly from the instrument readout. Scattering signals are observed on a PAR JB5 lock-in amplifier. The amplified reference signal of this instrument drives a mercury relay which modulates the potential of the control grid in the electron gun at 40 Hz. The output of the lock-in amplifier can be fed to the y axis of an X-Y recorder whose x-axis position is controlled by a sensing potentiometer which records the displacement of the detector from the beam axis. Alternatively, the output can be digitalized by a Vidar model 240 voltage-to-frequency converter and a scalar timer. The latter technique was used exclusively when making quantitative ratio measurements with and without spin analysis. The former technique is more convenient when obtaining angular distribution of the scattering cross sections.

VI. DIFFERENTIAL MEASUREMENTS

Differential scattering data were generally obtained with the oven displaced so that atoms are transmitted through the analyzer only if they have changed their spin state in the interaction region ("fields-on" condition). That is, the analyzer is normally set for extinction. With the analyzer inoperative, all atoms scattered within the angular range subtended by the detector are observed ("fields-off" condition).

The recoil angle corresponding to inelastic scat-

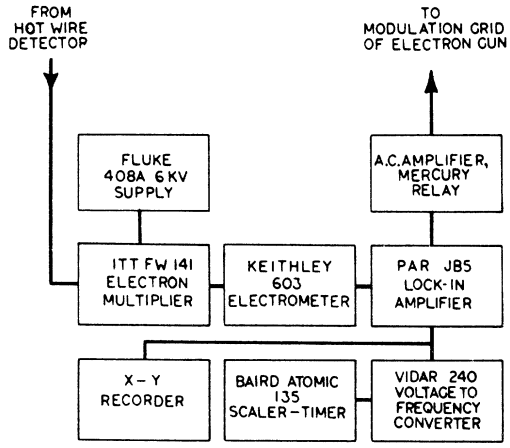

FIG. 2. Block diagram of detection system.

tering with energy loss E_0, to first order in α, is

$$\psi = \alpha\left[1 - (1 - E_0/E)^{1/2}\cos\theta\right],$$

where θ is the electron polar scattering angle. As in the elastic case, the finite detector height is taken into account by introducing an AFF γ'. For energies somewhat higher than E_0, γ' is strongly peaked at the displacement z corresponding to $\theta = 0$. As a consequence, the inelastic differential scattering signal exhibits a well-defined peak which reproduces the unscattered beam shape (see, for example, the 10-eV curve of Fig. 4 in RBGC). The displacement of this peak can be used to determine the mean atom speed or, assuming this is known, can serve as an independent calibration of the electron energy scale.

A typical differential scattering signal at 0.5 eV is shown in Fig. 3, under "fields-on" and "fields-off" conditions. These curves are roughly representative of the differential cross section, modified by the AFF, by the dispersions caused by finite spreads in electron and atom speed distributions, by finite beam widths, and by other instrumental effects. The peak at large angles is attributable partly to a rise in the cross section at these angles and partly to the increase in AFF to unity at $\theta = \pi$.

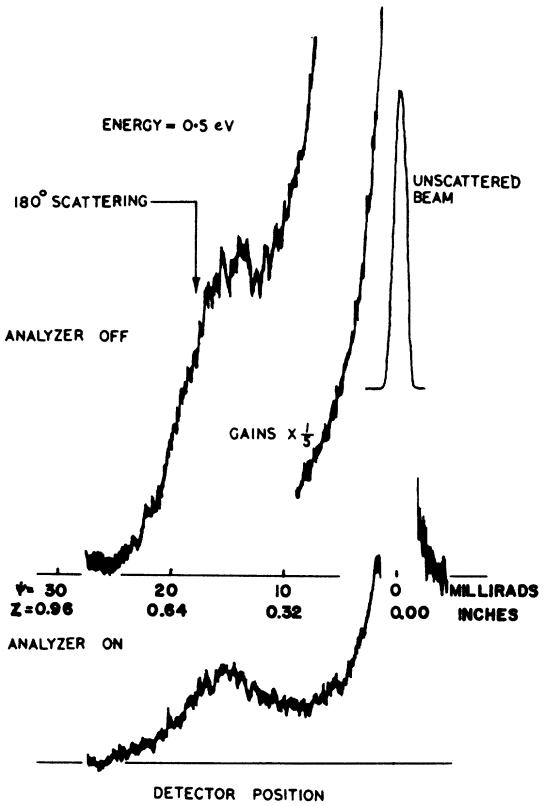

FIG. 3. Typical differential scattering signal. Electron energy is 0.5 eV. Upper and lower curves refer to "fields-off" and "fields-on" conditions, respectively. Abscissa is displacement of detector from beam axis, and equivalently, atom recoil angle ψ.

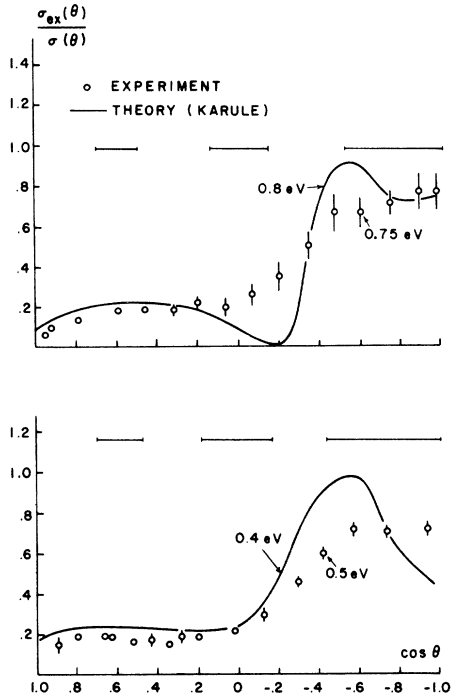

FIG. 4. Measurements of ratio $\sigma_{ex}(\theta)/\sigma(\theta)$ at 0.5 and 0.75 eV compared to theoretical values of Karule at 0.4 and 0.8 eV. The horizontal error bars are indicative of the over-all apparatus angular resolution.

With the detector set at a particular displacement, measurements of the ratio of the scattering signal with the analyzer fields on to that with the fields off yields the ratio $\sigma_{ex}(\theta)/\sigma(\theta)$. Experimental values of this ratio are shown in Figs. 4 and 5 at four different electron energies. These data have been corrected for the analyzer transmission factor and the beam residual depolarization as outlined in Appendix A. Note that, as discussed in Sec. II, geometry factors and the AFF corrections cancel in this determination. Of course the measured ratios still represent averages over the various distribution functions which yield an uncertainty in the polar scattering angle. Horizontal error bars in Figs. 4 and 5 indicate the approximate magnitude of this uncertainty. The vertical error bars refer to statistical error, representing two standard deviations.

These data exhibit the same general behavior at all energies. The ratio is small at small angles and large at large angles. This is to be expected from simple physical arguments, since atoms scattered through larger angles correspond to collisions with smaller impact parameters on the average, where exchange contributions should be

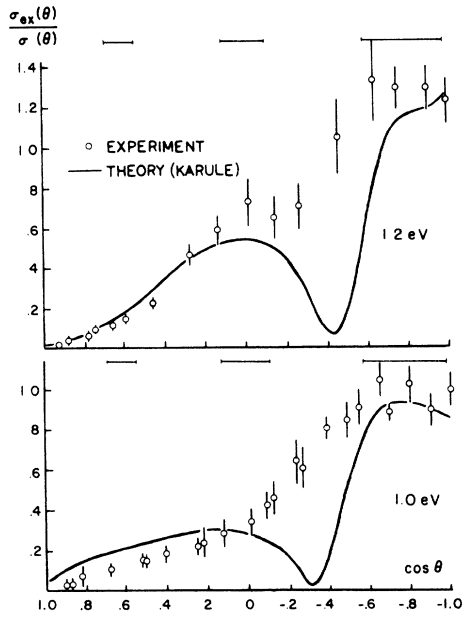

FIG. 5. Measurements of ratio $\sigma_{ex}(\theta)/\sigma(\theta)$ at 1.0 and 1.2 eV compared to theoretical values of Karule. The horizontal error bars are indicative of the over-all apparatus angular resolution.

important.

A small reproducible peak occurs in the 1.2-eV data at $\cos\theta \approx 0$. This can be attributed to a "spin-flip" signal caused by inelastic scattering from the high-energy tail of the electron energy distribution ($4\,^2S_{1/2}$-$4\,^2P_{1/2,3/2}$ transition). At the threshold for any inelastic transition the atom recoil angle corresponds to 90° elastic scattering, i.e., $\cos\theta = 0$. Moreover, at threshold the inelastic AFF is unity, i.e., all inelastic events are observed, whereas the corresponding form factor for elastic events is a minimum at $\theta = 90°$ [in our apparatus $\gamma(90°) \simeq 0.05$ at 1.2 eV]. Inelastic collisions at the ^2P threshold have a spin-flip probability of $\frac{4}{9}$ (see RBGC). For these reasons, even a small number of inelastically scattered atoms would give a relatively large effect, as observed.

Elastic differential cross sections, obtained by applying the formulas discussed in Sec. II to the raw scattering data, are shown in Fig. 6. Rather than attempting evaluations of the geometry factors and beam parameters in Eq. (3), absolute values have been assigned by a normalization procedure. The 1.0-eV differential cross sections were integrated over all angles (making reasonable extrapolations to zero and π rad) and equated to an experimentally determined total cross-section measurement at 1.0 eV performed in transmission (see Sec. VII). An error of a factor of 2 in the extrapolation to 0 and π scattering angles would have changed the absolute values by less than 20%.

Differential exchange cross sections were obtained by multiplying the differential cross sections in Fig. 6 by the observed cross-section ratios of Figs. 4 and 5. Results are shown in Fig. 7. The various remarks concerning the extrapolations to small and large angles also apply here.

The error in these normalized cross sections is attributable primarily to this extrapolation technique and to statistics. The AFF error is quite small, owing to its relative insensitivity to scattering angle over most of the angular range of our experiment. The statistical error ranges from up to about ± 10% for the full differential data to about ± 20% for the differential exchange data. An over-all estimate of the error for both of these quantities is ± 25% and ± 27%, respectively, attributable to ± 20% (uncertainty in total cross section used in normalization), ± 10% (extrapolation error), ± 5% (AFF error), and ± 10% or ± 20% (statistical error).

The maximum possible value for the ratio $\sigma_{ex}(\theta)/\sigma(\theta)$ occurs when $\eta^T - \eta^S = \mathrm{mod}\,\pi$ and $|T|/|S| = \frac{1}{2}$, where η^T, η^S are the relative phases of T, S, respectively. With these values $\sigma_{ex}(\theta)/\sigma(\theta) = \frac{4}{5}$. Reference to Fig. 5 shows that this

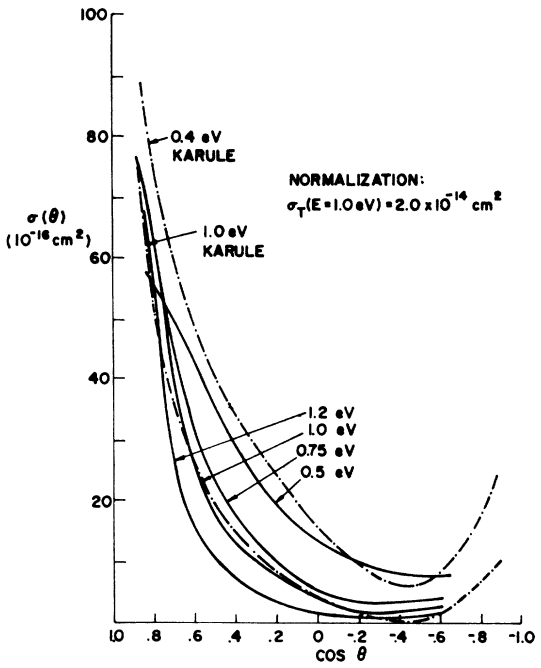

FIG. 6. Differential cross sections (solid curves) at 0.5, 0.75, 1.0, and 1.2 eV. Normalization is to the total cross section measured in transmission at 1.0 eV. Dot-dashed curves are theoretical values of Karule at 0.4 and 1.0 eV. The over-all error estimate in σ is ± 25%. The over-all error estimate in cos θ, defined as $\frac{1}{2}\Delta(\cos\theta)$, is ± 4% at $\cos\theta = 0.6$, ± 7% at $\cos\theta = 0$, ± 10% at $\cos\theta = -0.6$.

value is almost reached for $\cos\theta < -0.6$, i.e., for scattering angles greater than 145° at 1.0 and 1.2 eV.

Limited data for $\sigma_{ex}(\theta)/\sigma(\theta)$ can be obtained near the first inelastic threshold, since inelastic scattering close to threshold is spatially localized around angles corresponding to $\theta = 90°$ in elastic scattering. Experimental values for $\sigma_{ex}(\theta)/\sigma(\theta)$ corresponding to 180° elastic scattering are shown in Fig. 8 for electron energies up to 1.65 eV. A maximum occurs in this curve at an energy of 1.25 eV where the ratio very nearly reaches the theoretical limit.

VII. ABSOLUTE TOTAL CROSS-SECTION MEASUREMENTS

The total cross section is most conveniently obtained in a scattering-out mode. The detector is positioned on the center of the unscattered beam (beam axis). The scattering-out signal, i.e., the decrease in beam intensity observed with the electron gun operative, is proportional to the total collision cross section. Under certain simplifying assumptions the measured cross section σ is given by

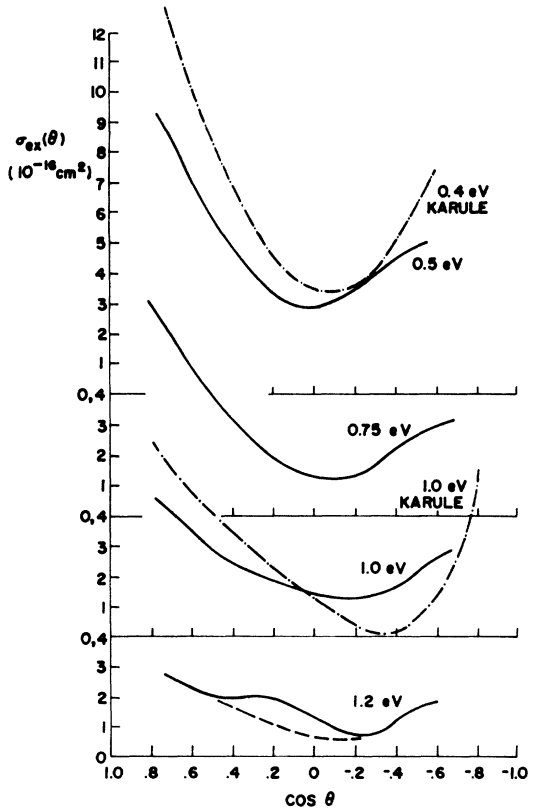

FIG. 7. Differential exchange cross sections (solid curves) at 0.5, 0.75, 1.0, and 1.2 eV. Dot-dashed curves are theoretical values of Karule at 0.4 and 1.0 eV. The over-all error estimate in σ is ±27%. The error estimate in $\cos\theta$ is the same as in Fig. 6.

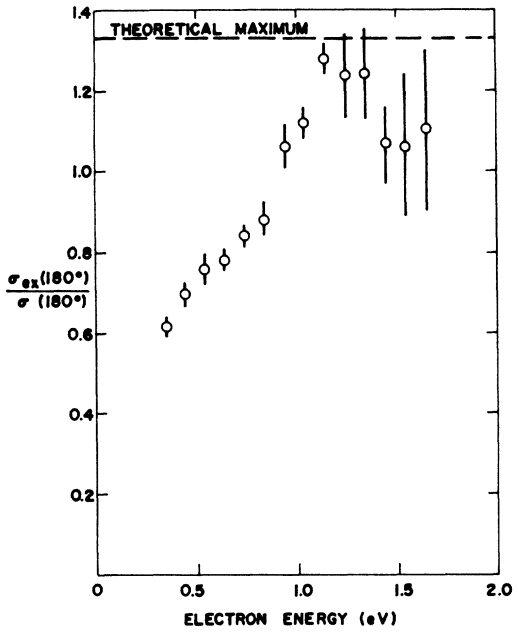

FIG. 8. $\sigma_{ex}(\theta)/\sigma(\theta)$ for $\theta = 180°$ (backward scattering) as a function of electron energy from 0.5 to 1.65 eV.

$$\sigma = I' h \langle V \rangle / I_a I_e , \tag{7}$$

where I_a, I_e are the atom and electron currents (particles/sec), I' is the scattering-out signal, h is the atom-beam height (i.e., the long dimension of the atom beam, assumed to be rectangular), $\langle V \rangle$ is the mean speed of the atom beam defined as

$$\langle V \rangle = \int f(V) V \, dV ,$$

where $f(V)$ is the normalized velocity distribution function of the beam in the interaction region.

The principal assumptions made in deriving Eq. (7) are the following: (a) The atom-beam density is uniform along both the beam-height dimension and along the beam axis. Its density may vary across the beam. (b) $\langle V \rangle$ is constant across the beam. (c) The entire collected electron beam crosses through the atom beam. It need not possess uniform density. (d) The angular resolution is independent of position along the beam axis. (This is a reasonable assumption if the length of the electron beam is very much less than L.)

Absolute cross sections can be obtained using Eq. (7) provided I' and I_a are measured using the same detector, and the *relative* gains of the current measurements of I' and I_a are known. The remaining quantities in Eq. (7) can be determined with reasonable accuracy. It is generally not practical to measure I_a in this experiment with the lock-in system; accordingly, a calibration was made to determine the relative gains by comparing scattering-out signals as observed by the dc beam electrometer and the phase-sensitive detector.

The atom-beam velocity was determined by observing the displacement of zero-angle inelastic recoil at energies above 10 eV, as described in Sec. III. Velocities obtained by this means are in good agreement with the value of the most probable velocity of a Maxwellian distribution corresponding to the measured source temperature.

The angular-resolution problem is discussed briefly in Appendix B in which estimates are made of both the angular efficiency and the errors resulting from the angular resolution in obtaining total cross sections using the recoil technique. It is shown that at 0.5 eV this error is about 1% and that it generally decreases with increasing energy. As a consequence, angular resolution does not contribute significantly to the over-all error in this experiment.

In both the differential and total cross-section measurements certain routine checks were performed to ensure proper operation of the electron gun. Chief among these was, first, the effect on scattering signal of the anode potential, and second, the linearity of the scattering signal vs gun current. When the anode potential V_a is close to the potential of the scattering region V_{sc} it is energetically possible for low-energy secondary electrons from the anode to reenter the scattering region. It was found necessary to operate with the anode at least 28 V more positive than the scattering region. Under this condition the scattering signal does not depend significantly upon the anode potential. At energies above 0.4 eV a linear relation between scattering signal and gun current was obtained, over a wide range of operating currents. Below 0.4 eV some nonlinearity was observed due to excessive space charge; it is primarily for this reason that we make no claim concerning the accuracy of our total cross-section data at energies below 0.4 eV. Examples of these routine checks are shown in Fig. 9 (effect of anode potential) and

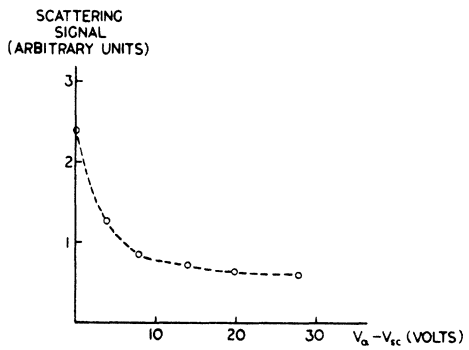

FIG. 9. Influence of anode potential upon "scattering" signal. Anode must be at least 28 V higher than the potential of scattering region to ensure that all electrons passing through scattering region are collected.

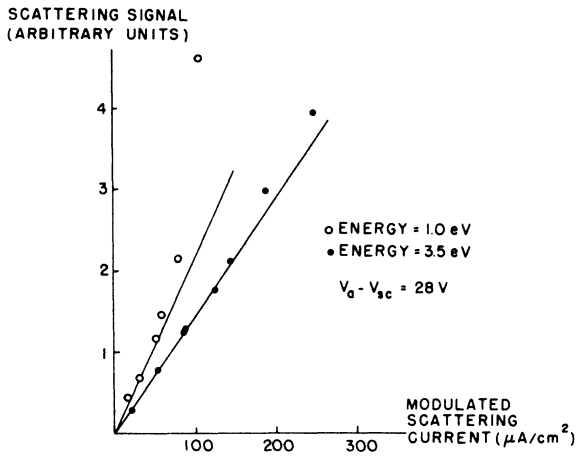

FIG. 10. Influence of space charge upon "scattering" signal. To ensure linearity of scattering signal vs gun current, the latter was always held below 50 μA/cm^2.

Fig. 10 (linearity check). The total cross-section measurements are shown in Fig. 11. Above the very low-energy region, the experimental cross sections lack pronounced structure. However, a small inflection at $E = 1.5$ eV was reproducibly observed in all the data. This is possibly indicative of a resonance at an energy just below the first excitation energy.

The maximum error in the absolute values of the total cross-section measurements is estimated to be $\pm 20\%$. The error arises mostly from the gain calibration of the lock-in amplifier (7%), from the variation in scattering signal with anode voltage (10%), and from the uncertainties in the beam height (6%) and in the atom velocity (4%). The relative shape of the total cross-section curve is estimated to be accurate to within 10% above 0.4 eV. Statistics (i.e., signal-to-noise ratios S/N) are quite favorable in the scattering-out mode despite the generally small fraction of the total beam which is scattered. Typical S/N for the integration times employed in the present work (several minutes per datum point) are of the order of 30. Modulation of the atom beam by scattering caused by gas liberated from the anode by the modulated electron beam could introduce serious error under certain conditions. This has indeed been observed. In the present case, with scattering currents of the order of 10 μA, this effect is completely negligible.

Values of the total and total exchange cross sections obtained by integrating the differential cross sections are shown in Table I. Table I also includes a comparison with total cross sections obtained from the scattering-out data and theoretical values of Karule (see Sec. VIII). In view of the very good agreement between the energy depen-

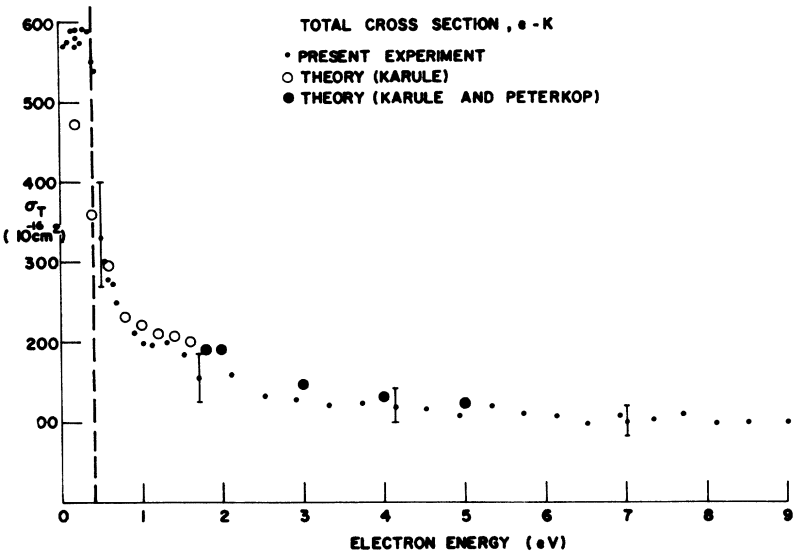

FIG. 11. Total cross sections for the scattering of low-energy electrons by potassium, compared to theoretical results of Karule (○) and Karule and Peterkop (●). Experimental values below 0.4 eV are of qualitative value only, primarily because of space-charge influence.

dence of the total cross sections obtained by integration and by scattering-out, it is reasonable to assume that the estimates made in extrapolating the differential data to 0 and π are not excessively in error. The error in extrapolation of the differential exchange data is expected to be even smaller since the exchange cross sections are much smaller than the full differential cross sections at small angles where most of the error arises. We estimate the error in the total exchange cross section to be ± 35%, consisting of normalization error (± 20%), integration error (± 20%), and extrapolation error (± 10%).

VIII. COMPARISON WITH PREVIOUS RESULTS

The early measurements of Rubin *et al.*[1] were not corrected for the finite detector height (AFF). When this is done the two sets of measurements are in good agreement over the range of overlap ($20° < \theta < 60°$). Differential exchange cross sections have not previously been reported.

The absolute values of the total cross sections are a factor of about 2 smaller than those obtained by Brode,[11] and furthermore do not reveal the pronounced structure of the Brode curve. The difficulties with the Brode data are discussed by Bederson[12] and in a forthcoming review article.[13]

Perel, Englander, and Bederson[14] performed measurements on lithium and sodium using the recoil technique. These were relative determination normalized to Brode's potassium data. Several attempts to obtain absolute values of total cross sections at 13 eV were also made here, including potassium as well. It is believed that these values are in error due to inadequate shielding from secondary and reflected electrons.[13] (Renormalization of the lithium and sodium data to the present results is discussed in Ref. 15.)

Recently, Rubin and co-workers[16] have performed similar total cross-section measurements using the recoil technique in transmission (scattering-out). Their potassium results are in good agreement with ours, although the Rubin *et al.* absolute values are slightly higher than those reported here. The other alkalis studied by them (rubidium and cesium) exhibit similar behavior, that is, are roughly half the Brode values, and do not possess structure.[17]

TABLE I. Summary of total elastic and exchange cross sections from theory (Karule) and present experiment. The error estimate for σ_{ex} is ± 35%. Units are 10^{-16} cm^2.

Energy (eV)	σ (from scattering-out data)	σ(from integration of differential cross sections)	σ_{ex} (from integration of differential cross sections)	Energy (eV)	σ(theory)	σ_{ex}(theory)
0.5	260 ± 40	270	63	0.4	350	113
0.75	230 ± 30	220	41	0.6	290	72
1.0	200 ± 30	200[a]	33	0.8	260	53
				1.0	240	45
1.2	180 ± 30	190	21	1.2	220	32

[a]Normalized to scattering-out data.

The upper and lower bounds set by Rubin *et al.*[1] were obtained by normalization to Brode's total cross sections. When renormalized to the present values these bounds are satisfied by the values presented in Table I. Total exchange cross sections for electron-alkali collisions as measured by optical-pumping techniques are generally found to be of the order of $2\times10^{-14}\,\mathrm{cm}^2$. This is not considered to be in disagreement with the present results since the optical-pumping values generally pertain to a lower-energy region than that reported here.

The results of electron-alkali scattering calculations have been shown to be very sensitive to the inclusion of exchange, and to the particular form of the polarization potential used.[18] As a consequence, adiabatic calculations based upon an interaction potential, even including exchange, will show quite varied behavior in the low-energy domain studied in the present work. The use of close coupling has not been extensively employed in the alkalis, although one should expect that elastic scattering should be reasonably well described in a two-state expansion involving only nS, nP states provided accurate wave functions are used. This is due to the fact that the dipole polarizability which contributes so heavily to the scattering process in the alkalis at low energies is attributable almost completely to the dipole matrix element which couples nS-nP. Thus the oscillator strengths for the resonance transition, which are determined by this same matrix element, are very nearly equal to unity in all of the alkalis.[19]

Karule and Karule and Peterkop[4] have performed such two-state calculations for Li, Na, K, and Cs. They employed semiempirical wave functions for potassium with closed-shell potentials determined by Gaspar's method.[20] It is primarily with these calculations that we compare our results. Karule and Peterkop calculated elements of the R matrix for several energies from the $4S$-$4P$ threshold to 5 eV. The first nine partial waves were included, with exchange included in the first four. They also calculated the $4S$-$4P$ excitation cross section from the same R matrix, and as a consequence obtain values for the *total* cross section, to which we can directly compare our results (this neglects, of course, contributions from other inelastic channels). Karule extended this work below threshold to obtain elastic phase shifts; here up to eight partial waves (at threshold) were included, and exchange was taken into account for the lower partial waves (up to $L=3$).

The Karule values of $\sigma_{ex}(\theta)/\sigma(\theta)$, as well as $\sigma_{ex}(\theta)$ separately, are shown in Figs. 4–7 along with our results. The deviations between theory and experiment around $\cos\theta=0$ are not considered serious since the theoretical maxima and minima arise when the respective cross sections get very small due to cancellation between the several partial waves involved. A small error in the phase shifts will substantially change the shape of the curves in this region. Moreover, since the cross sections in this region are very small the experimental results are strongly affected by scattering through other angles, as a consequence of the spreads in the electron and atom velocity distributions. The approximate magnitude of the error introduced by these spreads is shown by the horizontal error bars in Figs. 4 and 5. Agreement of theory and experiment in the absolute differential cross-section curves (Figs. 6 and 7) is quite good considering the experimental and theoretical uncertainties.

The Karule and Karule-Peterkop total cross sections (including $4S$-$4P$ excitation) are shown along with the experimental values in Fig. 11. Again the relative shapes and absolute values are in good agreement.[15]

ACKNOWLEDGMENTS

We thank Professor H. H. Brown, Professor T. M. Miller, and Professor K. Rubin for their invaluable assistance throughout the course of this work. The contributions of Dr. P. Eisner and Dr. R. Celotta, J. DeSantis, J. Ofenleger, and A. Riederer are also gratefully acknowledged.

APPENDIX A: CORRECTIONS TO RATIO MEASUREMENTS FOR RESIDUAL DEPOLARIZATION AND FOR TRANSMISSION OF ANALYZER

We assume (a) that the analyzer removes all the atoms of spin state $\alpha(\uparrow)$ and transmits a fraction T of atoms of spin state $\beta(\uparrow)$, and (b) that the composition of the beam is symmetric for equal oven displacements on either side of the beam axis (the intensities need not be equal). Let D be the residual depolarization. Figure 12 shows the various beam constituents before and after polarization and analysis without scattering [Fig. 12(a)], and with scattering [Fig. 12(b)]. The total current entering the polarizer is I' or I''. Setting the oven to the right (up in the figures) selects the $\beta(\uparrow)$ state. This setting is used to measure T. The *observed* transmission T_0 (usually of the order of 80% in our apparatus) is

$$T_0 = IT(1-D)/I = T(1-D)\ . \tag{A1}$$

Setting the oven to the left (down in the figure) selects the $\alpha(\uparrow)$ state and is used to measure D. The *observed* residual depolarization D_0 is

$$D_0 = TD\ . \tag{A2}$$

Scattering data are taken with the oven displaced to the left so that the analyzer is then set for extinction. At a given scattering angle a fraction S of the incident atoms are scattered and a fraction R

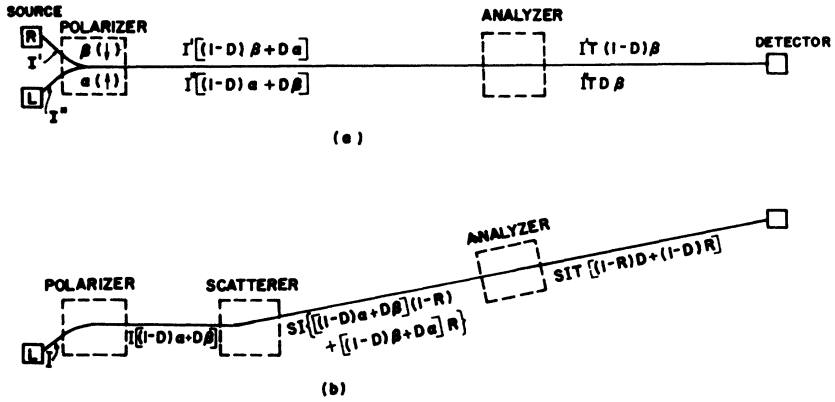

FIG. 12. Diagram illustrating various beam constituents (a) without and (b) with scattering. See text of Appendix A.

of these change their spin state as a result of collisions. The composition of the scattering signal with and without spin analysis is shown in Fig. 12(b). The observed spin-flip ratio R_0 is related to the actual ratio R by

$$R_0 = TD(1-R) + T(1-D)R \ . \tag{A3}$$

Using Eqs. (A1) and (A2) we obtain

$$R = (R_0 - D_0)/(T_0 - D_0) \ . \tag{A4}$$

APPENDIX B: ANGULAR RESOLUTION IN TOTAL ELASTIC CROSS-SECTION MEASUREMENT

The average angular efficiency $\bar{\eta}(\theta)$ in a recoil experiment using rectangular geometry has been calculated by Eisner,[21] who shows that

$$\bar{\eta}(\theta) \simeq \bar{\eta}_y(\theta) + \bar{\eta}_z(\theta) - \bar{\eta}_y(\theta)\bar{\eta}_z(\theta) \ , \tag{B1}$$

where $\bar{\eta}_y(\theta)$ and $\bar{\eta}_z(\theta)$ are the average efficiencies assuming a one-dimensional beam with infinite extent in the z and y directions, respectively. To estimate the error caused by infinite angular resolution in the present experiment we will neglect the contribution of $\bar{\eta}_y$, which is equivalent to assuming that the atom beam possesses infinite height. This calculation will thus overestimate the resolution error, which we shall show, in any case, is small compared to other systematic effects.

Eisner shows that

$$\bar{\eta}_z(\theta) = -(w-a)/2a + (L\bar{\alpha}/2a)\theta^2 \ , \tag{B2}$$

where w = beam width at detector, a = beam width in the interaction region, $\bar{\alpha} = mv/MV = 0.0177\sqrt{E}$ for potassium at 550 °K, mv, MV = electron and atom momentum, respectively, E = electron energy in eV, and L = distance from interaction volume to detector.

This calculation assumes a monoenergetic atom beam possessing the most probable beam velocity of an effusive source at temperature T. In the present experiment $w = 0.016$ in., $a = 0.008$ in., $L = 32.000$ in. The efficiencies as a function of angle, under the above assumptions, are approximate step functions at 6° for 9 eV, 9.5° at 1.2 eV, and 11.5° at 0.5 eV.

The relative error Δ in the measured total cross section caused by the finite resolution is

$$\Delta = [\int_0^{\theta_0} \sigma(\theta)\sin\theta\, d\theta - \int_0^{\theta_0} \bar{\eta}(\theta)\sin\theta\, d\theta]/\sigma \ , \tag{B3}$$

where σ is the total elastic cross section and θ_0 is the smallest θ for which $\bar{\eta}(\theta) = 1$. To estimate Δ we calculate $\sigma(\theta)$ from the Karule phase shifts (Fig. 6); for all cases $\Delta \approx 1\%$ or less.

---

†Research supported by the Army Research Office, Durham, N. C., Grant No. DA-ARO-D-31-124-G1109, the National Science Foundation Grant No. GP-17193-NSF, and the Air Force Office of Scientific Research Grant No. AFOSR-69-1672.

*Part of a thesis presented by Richard E. Collins in partial fulfillment of the requirements for the Ph. D. degree at New York University.

‡Present address: A. W. A. Physical Laboratory, 348 Victoria Road, Rydalmere, New South Wales, Australia.

§Address after July 1971: Physics Department, New York University, 2 Washington Place, New York, N. Y. 10003.

‖Present address: Bell Telephone Laboratories, Whippany, N. J. 07981.

[1]K. Rubin, J. Perel, and B. Bederson, Phys. Rev. 117, 151 (1960).

[2]*Methods of Experimental Physics*, edited by B. Bederson and W. L. Fite (Academic, New York, 1968), Vol. 7A, pp. 89–95.

[3]D. E. Pritchard, G. M. Carter, F. Y. Chu, and D. Kleppner, Phys. Rev. A 2, 1922 (1970); D. Pritchard, D. Burnham, and D. Kleppner, Phys. Rev. Letters 19, 1363 (1967); Abstracts of Papers of the International Conference on Atomic Physics, New York University, 1968, p. 147 (unpublished).

[4]E. M. Karule and R. K. Peterkop, in *Atomic Collisions III*, edited by Y. Ia. Veldre (Latvian Academy of Sciences, Riga, USSR, 1965) [JILA Information Center Report No. 3, University of Colorado, Boulder, Colo. (unpublished)], pp. 1–27; E. M. Karule, *ibid.*, pp. 29–48.

[5]Preliminary publications relating to the present work include the following: angular distributions: R. E. Collins, M. Goldstein, B. Bederson, and K. Rubin, Phys. Rev. Letters 19, 1366 (1967); Phys. Letters 27A, 440 (1968); *Proceedings of the Sixth International Conference on the Physics of Electronic and Atomic Collisions* (MIT Press, Cambridge, Mass., 1969), p. 681; *Physics of the One- and Two-Electron Atoms*, edited by F. Bopp and H. Kleinpoppen (North-Holland, Amsterdam, 1969), p. 642; total cross sections: R. E. Collins, B. Bederson, M. Goldstein, and K. Rubin, Bull. Am. Phys. Soc. 14, 251 (1969).

[6]K. Rubin, B. Bederson, M. Goldstein, and R. E. Collins, Phys. Rev. 182, 201, (1969).

[7]B. Bederson and K. Rubin, AEC Technical Report No. NYO-10, p. 117, New York University (unpublished).

[8]B. Bederson, J. Eisinger, K. Rubin, and A. Salop, Rev. Sci. Instr. 31, 852 (1960).

[9]R. E. Collins, B. B. Aubrey, P. N. Eisner, and R. Celotta, Rev. Sci. Instr. 41, 1403 (1970).

[10]R. E. Collins, Ph.D. thesis (New York University, 1968) (unpublished).

[11]R. B. Brode, Phys. Rev. 34, 673 (1929).

[12]B. Bederson, Comments At. Mol. Phys. 1, 135 (1970); 2, 7 (1970).

[13]B. Bederson and L. J. Kieffer (unpublished).

[14]J. Perel, P. Englander, and B. Bederson, Phys. Rev. 128, 1148 (1962).

[15]The total electron-potassium cross sections reported here affect the absolute electron-lithium and-sodium values of Perel *et al.* (Ref. 11). In that work relative cross sections were normalized to the Brode potassium cross sections. Renormalization to the present potassium cross sections places them in considerably better agreement with the Burke and Taylor calculations. The renormalized results for lithium and sodium can be obtained by writing to the present authors.

[16]K. Rubin (private communication).

[17]It should be noted, however, that O. B. Shpenik, A. N. Zavilopulo, I. S. Aleksakhin, and I. P. Zapesochny [*Abstracts of Papers of the Sixth International Conference on Physics of Atomic and Electronic Collisions* (MIT Press, Cambridge, Mass., 1969), p. 260] have reported preliminary results of a crossed-beam electron-attenuation experiment for cesium in which a very large bump appears at about 2 eV. Absolute values were not presented; the electron energy spread was between 0.15 and 0.5 eV.

[18]M. H. Mittleman, Phys. Rev. 147, 69 (1966).

[19]B. Bederson and E. J. Robinson, in *Molecular Beams, Advances in Chemical Physics*, edited by J. Ross (Interscience, New York, 1966), Vol. X, pp. 1–27.

[20]R. Gaspar, Acta Phys. Acad. Sci. Hung. 2, 151 (1952).

[21]P. N. Eisner, Ph.D. dissertation (New York University, 1969) (unpublished).

PHYSICAL REVIEW A VOLUME 3, NUMBER 6 JUNE 1971

Born Wave Cross-Section Calculations for Collisional Quenching of Metastable H(2*s*) by Helium, Neon, Argon, and Krypton†

H. Levy II
Smithsonian Astrophysical Observatory, Cambridge, Massachusetts 02138
and Harvard College Observatory, Cambridge, Massachusetts 02138
(Received 7 December 1970)

Total quenching cross sections for metastable H(2*s*) atoms in collisions with helium, neon, argon, and krypton have been calculated over the incident-energy range 1.0 keV–1.6 MeV in the first Born approximation with the added approximation of closure used to describe target excitation. The first-Born-approximation cross sections for helium target atoms are one-third the measured values of Byron, Krotkov, and Medeiros over the incident-energy range 1.0–5.0 keV. The first-Born-approximation results for the heavier targets are much larger than experiment, although scaled results based on parameters determined from electron-loss data for H(1*s*) show fair agreement with recent experiments. The contributions of individual quenching processes are examined, and electron loss dominates for incident energies greater than 4.0 keV.

I. INTRODUCTION

To determine the contributions of individual quenching channels such as excitation, deexcitation, and ionization to the total quenching cross section and the dependence of these contributions on the heavy-particle relative velocity, first-Born-approximation calculations of the total quenching cross sections for metastable H(2*s*) in collision with helium, neon, argon, and krypton target atoms have been performed. The results for helium are reported in detail and compared with the recent measurements of Byron, Krotkov, and Medeiros.[1]

II. THEORY

Derivations of the two basic cross-section formulas have been discussed earlier by Levy.[2] Atomic units are used throughout.

The cross section for the particular quenching process in which the target is not excited and the